

# Testing the beamed inverse-Compton model for jet X-ray emission: velocity structure and deceleration?

M.J. Hardcastle

*School of Physics, Astronomy and Mathematics, University of Hertfordshire, College Lane, Hatfield, Hertfordshire AL10 9AB*

18 November 2018

## ABSTRACT

By considering a small sample of core-dominated radio-loud quasars with X-ray jets, I show, as has been argued previously by others, that the observations require bulk jet deceleration if all of the X-ray emission is to be explained using the widely adopted beamed inverse-Compton model, and argue that jets even in these powerful objects must have velocity structure in order to reconcile their radio and X-ray properties. I then argue that the deceleration model has several serious weaknesses, and discuss the viability of alternative models for the decline in X-ray/radio ratio as a function of position. Although inverse-Compton scattering from the jets is a required process and must come to dominate at high redshifts, adopting an alternative model for the X-ray emission of some nearby, well-studied objects can greatly alleviate some of the problems posed by these observations for the beamed inverse-Compton model.

**Key words:** galaxies: active – X-rays: galaxies – galaxies: jets – radiation mechanisms: non-thermal

## 1 INTRODUCTION

### 1.1 X-ray jets and the beamed inverse-Compton model

X-ray emission from the jets of radio-loud active galaxies is now known to be common. In the low-power, Fanaroff & Riley (1974) type I (FRI) objects, objects that have detectable jets in the radio often (Worrall, Birkinshaw & Hardcastle 2001) and perhaps even always (Hardcastle et al. 2002b) have corresponding X-ray jet emission, although the X-ray/radio ratio varies widely. Because of the continuity between the radio, optical and X-ray spectra in the best-studied jets (e.g. Wilson & Yang 2002; Hardcastle, Birkinshaw & Worrall 2001) the X-ray emission is argued to be synchrotron; the broad-band spectra of the jets can be fitted with one-zone synchrotron models (i.e., models with a single population of relativistic electrons with  $N(E)$  monotonically decreasing as a function of  $E$ ), although neither these broad-band spectra (e.g. Hardcastle et al. 2001) or their detailed properties (e.g. Hardcastle et al. 2003, Perlman & Wilson 2005) are consistent with standard continuous-injection models for the particle acceleration. The X-ray emission must then trace high-energy particle acceleration (electron Lorentz factors  $\gamma \gtrsim 10^7$ ). It is coincident, in the best-studied cases, with the region where strong bulk deceleration is thought to be taking place (Hardcastle et al. 2002b), and is thus limited to the inner few kpc corresponding to the one-sided (relativistically beamed) inner part of the jet, although in at least one case, NGC 6251, X-ray synchrotron emission plausibly persists out to 100-kpc scales (Evans et al. 2005).

It is much less clear that a single mechanism can explain X-ray jet emission from the more powerful FR II objects. In some low-power FR II radio galaxies, jet X-rays are plausibly modelled as

synchrotron emission (e.g. 3C 219, Comastri et al. 2003; 3C 403, Kraft et al. 2005; Pictor A, Hardcastle & Croston 2005). But the most widely studied class of objects to exhibit X-ray jets, following the discovery of the prototype, PKS 0637–752 (Schwartz et al. 2000), are core-dominated quasars (CDQ), and these often have broad-band spectra in which the optical data points preclude a one-zone synchrotron model. Nor is it possible to explain the properties of the jets as a result of inverse-Compton scattering of synchrotron photons (synchrotron self-Compton, SSC) or cosmic microwave background photons (CMB/IC) if the jet is non-relativistic and the magnetic field strength in the jet is close to equipartition, although such models, with fields close to equipartition, successfully explain the X-ray emission from other components of powerful radio sources, such as hotspots and lobes (see Hardcastle et al. 2004, Kataoka & Stawarz 2004, Croston et al. 2005, and references therein, for discussions of these components). Instead, the model proposed independently by Tavecchio et al. (2000) and Celotti et al. (2001) is widely adopted. In this model, the jet is moving relativistically, with a bulk Lorentz factor  $\Gamma$ . As seen by the jet, the energy density in the microwave background increases by a factor of the order  $\Gamma^2$ , and this increases the emissivity of the CMB/IC process in the jet frame. Both because the jet-frame inverse-Compton emissivity is anisotropic (the CMB is anisotropic in the jet frame) and because of the strong beaming in the lab frame at high bulk Lorentz factors, this process is only viable in objects where the jet velocity vector makes a small angle to the line of sight: however, we know from superluminal motion observations that this is true of the CDQ population. A key result of these early analyses of PKS 0637–752 was that the angle to the line of sight, and the bulk Lorentz factor  $\Gamma$ , were consistent with constraints on the pc-scale speed from super-

luminal motion observations. Thus the model implied little or no bulk deceleration between the parsec and 100-kpc scales in these jets, a point emphasised by Tavecchio et al. (2004).

## 1.2 Problems with the model

Since this beamed CMB/IC model (hereafter just referred to as the CMB/IC model) was first proposed a number of objections to it have been put forward which to some extent undermine the original strong arguments for its adoption. These can be summarized as follows:

- (i) Incompatibility with jet speeds from radio observations
- (ii) The inherent unlikelihood of one-zone models
- (iii) Fine-tuning of  $\gamma_{\min}$
- (iv) Differences between X-ray and radio structures
- (v) Radio/X-ray ratio changes

I discuss them in detail in the following subsections.

### 1.2.1 Jet speeds from radio observations

The kpc-scale jet bulk speeds required in the CMB/IC model are inconsistent with the best constraints available using jet sidednesses and prominences derived from radio observations of lobe-dominated radio galaxies and quasars (Bridle et al. 1994; Wardle & Aaron 1997; Hardcastle et al. 1999; Arshakian & Longair 2004; Mullin et al., in prep.). The best-fitting characteristic speeds derived in these papers (which use varying samples and analysis methods) are in the range  $0.5\text{--}0.7c$ , and bulk Lorentz factors as high as 10 are definitely incompatible with the observations (Mullin et al., in prep.). As the samples used for this sort of work are generally lobe-dominated objects (they must be drawn from samples whose orientation to the line of sight is unbiased, or at least where the bias is understood, in order to allow the statistical inference of the jet speed), one could argue that the CDQ are physically different (which would be inconsistent with unified models), or that they represent a tail of objects with extremely high jet speeds (which would render them effectively irrelevant for understanding the physics of radio sources in general), but these positions clearly have disadvantages.

The best way to reconcile the radio observations with the beamed CMB/IC model without invoking differences between the population of X-ray-jetted CDQ and the population of radio sources in general is to suppose that the jet has some velocity structure, in the sense that a cross-section of the jet at any given distance from the nucleus contains material moving away from the nucleus at different speeds. A simple model, for the sake of discussion, would be one in which the jet in all powerful sources consisted of a slow outer sheath (with  $v/c \sim 0.5$ ) and a fast central spine (with  $\Gamma \sim 10$ ). Doppler dimming would then prevent any detection of the spine in the lobe-dominated objects used for the radio-based speed detections. The spine would dominate at small angles to the line of sight, and be responsible for the X-ray jet emission of CDQ via the CMB/IC process. Conceivably the sheath could produce X-rays via the synchrotron process too, as seen in some lobe-dominated objects (see above). The consequences of this spine-sheath model will be discussed later in the paper.

### 1.2.2 Synchrotron emission and one-zone models

The argument for rejecting synchrotron emission as the mechanism for the X-rays is based on the assumption that synchrotron emission would be described by the kind of one-zone model discussed

above (a single electron population with monotonically decreasing  $N(E)$ ). There are two reasons why arguments based on this assumption should be treated with caution. One is the fact (pointed out by Dermer & Atoyan 2002) that  $N(E)$  need not monotonically decrease: electron losses against the microwave background can produce dips in the energy spectrum. The other, simpler point is that we have good reasons to suppose that a single electron population *cannot* describe a kpc-scale region emitting by the X-ray synchrotron process. The loss timescale for X-ray-synchrotron-emitting electrons in the magnetic field strength appropriate for a jet is of the order of tens of years at most, so such electrons can travel at most tens of light years from their acceleration site: a spatially uniform electron population is therefore not possible unless the acceleration mechanism is uniformly distributed. The nearest radio galaxy, Cen A, in which the resolution is matched to those spatial scales, clearly shows multiple discrete acceleration sites (e.g. Hardcastle et al. 2003)<sup>1</sup>. If synchrotron emission in more distant objects were to follow this pattern, our X-ray flux measurements, with a spatial resolution of order  $10^3$  times the loss spatial scale, are averaging over a number of different electron populations, and the resulting effective spectrum need not, and in general will not, resemble a one-zone model. As discussed above, the net spectrum of the X-ray jet region in FRI radio galaxies is often reasonably well fitted with a one-zone model (one with *ad hoc* assumptions about the high-energy slope); but we cannot assume that the same will be true of more powerful jets, which presumably have very different physics and particle acceleration mechanisms.

### 1.2.3 Fine-tuning of $\gamma_{\min}$

The lowest possible Lorentz factor of the electrons plays a crucial role in the CMB/IC model. To scatter CMB photons ( $T = 2.7(1+z)$  K in the frame of the active nucleus) into the X-ray (1 keV, lab-frame) requires electrons with energies of order  $10^3$ , since the energy gain in the inverse-Compton process goes as  $\gamma^2$ . But if relativistic boosting is important this constraint becomes  $\gamma_{\min} \sim 10^3/\Gamma$  (if we make the approximation  $\Gamma \sim \mathcal{D}$ , where  $\mathcal{D}$  is the Doppler factor). In fact we require  $\gamma_{\min}$  to be significantly less than this, since we require the CMB/IC spectrum to peak below 1 keV (otherwise a flat or even inverted X-ray spectrum would be observed). At the same time, depending on the low-energy electron energy spectrum assumed (and it is important to bear in mind that these calculations require an enormous extrapolation from the observable electron energies: e.g. Harris 2004), there may be a *lower* limit on  $\gamma_{\min}$  from the requirement that the CMB/IC prediction should not exceed the observed optical flux density of the jet, and there is a definite limit on the number of cold ( $\gamma \approx 1$ ) electrons from bulk Comptonization of the CMB (Georganopoulos et al. 2005) which in the case of PKS 0637–752 may provide a stringent constraint (Uchiyama et al. 2005). Depending on the models and assumptions used, these different constraints may require very fine tuning of  $\gamma_{\min}$ . In addition, the  $\gamma_{\min}$  values commonly used,  $\sim 20$ , are significantly different from the best estimates of  $\gamma_{\min}$  derived from radio observations of hotspots,  $\gamma_{\min} \sim 500$  (see e.g. Hardcastle 2001).

<sup>1</sup> M. Lyutikov has pointed out to me that this type of fine spatial structure in electron populations is also seen in pulsar wind nebulae, such as the Crab (e.g. Bietenholz et al. 2004).

### 1.2.4 X-ray and radio knots

Tavecchio, Ghisellini & Celotti (2003) pointed out that, since the X-ray emission in the CMB/IC model traces very low-energy electrons ( $\gamma \sim 10$ ) we would expect it to vary spatially much more smoothly than the radio or optical emission, which traces higher-energy electrons with shorter radiative lifetimes ( $\gamma \sim 10^4\text{--}10^6$ ) and which also depends on the magnetic field strength. In fact, knots in jets such as that in 3C 273 show similar sizes in the X-ray, radio and optical. Tavecchio et al. propose to solve this problem by suggesting that such knots are composed of many unresolved subclumps, but, as pointed out by Stawarz et al. (2004), allowing a low filling factor makes SSC a viable process again. Similarly, we would not expect to see positional offsets between radio and X-ray peaks, since a peak in the X-ray should represent an increase in the normalization of the electron energy spectrum, and so coincide with increased radio brightness, but such offsets are observed in some CDQ jets (e.g. Siemiginowska et al. 2002).

### 1.2.5 Radio/X-ray ratio changes

Some quasars show a significant change in the radio/X-ray flux ratio as a function of distance along the jet, almost always in the sense that there is less X-ray emission for a given amount of radio emission further from the nucleus. This is seen in samples of objects (e.g. Sambruna et al. 2004) as well as in individual well-studied objects such as 3C 273 (Marshall et al. 2001; Sambruna et al. 2001). Georganopoulos & Kazanas (2004) have argued, following earlier suggestions, that in the CMB/IC model this can be understood as a deceleration of the jet. This suggestion will be tested, and its consequences explored, in later sections of the present paper.

## 1.3 This paper: testing the model

The list of potential problems presented above makes it clear that a critical test of the CMB/IC model for quasar jets is urgently needed. Possible tests fall into two categories: statistical, large-sample tests and tests that involve the details of particular observations. One promising approach in the former category is to look for a correlation between the jet X-ray/radio ratio and the energy density of the CMB, which increases as  $(1+z)^4$ . So far no correlation has been found (Marshall et al. 2005) which, in the framework of the CMB/IC model, implies that there must be a wide range in the jet beaming parameters. If this is the case, the assembly of a sample large enough to test the model may take a very long time (and will certainly be dependent on the award of a large amount of further *Chandra* time). Similarly, it would be desirable to see whether the distribution of angles to the line of sight required by the CMB/IC model is compatible with the statistics of the CDQ with respect to their parent population of unbeamed objects, but at present the CDQ showing X-ray jets are a heterogeneous population drawn from different parent populations with different selection criteria, and a test of the model in this way would probably require new samples to be defined and observed.

As existing observations do not allow a statistical approach, I concentrate in this paper on the results that can be inferred from detailed observations of individual objects, and in particular from the observation that many jets have X-ray/radio flux ratios that are a strong function of position (Section 1.2.5). I construct a small sample of well-resolved jets and make measurements and infer jet properties in a systematic way. The results allow some conclusions

to be drawn about the properties of jet speeds if the CMB/IC model is correct, and motivate further consideration of alternative models.

In what follows I use a concordance cosmology with  $H_0 = 70$  km s<sup>-1</sup> Mpc<sup>-1</sup>,  $\Omega_m = 0.3$  and  $\Omega_\Lambda = 0.7$ . Spectral indices  $\alpha$  are the energy indices and are defined in the sense that flux  $\propto \nu^{-\alpha}$ . The bulk Lorentz factor of a jet is always denoted  $\Gamma$ , while  $\gamma$  is used for the random Lorentz factor of electrons.

## 2 SAMPLE AND ANALYSIS

The sample of objects analysed here was taken from the XJET catalogue (<http://hea-www.harvard.edu/XJET/>), maintained by Harris, Cheung & Stohman, as it stood at June 2005. This catalogue aims to maintain an up-to-date list of objects for which jet- or hotspot-related X-ray emission has been claimed in the literature. I selected from this list FR II objects with X-ray jet detections that are not clearly described as synchrotron emission, that show extended structure, e.g. an extended jet or multiple knots, and that have useful radio data available in the Very Large Array (VLA) archive. The final sample consisted of 9 objects of which all but one (Pic A) were quasars: Pic A is of course a broad-line radio galaxy and so probably a low-luminosity counterpart of a quasar. Although there are good arguments that the jet in Pic A is synchrotron in origin (Wilson, Young & Shopbell 2001; Hardcastle & Croston 2005) I retained it in the sample, as it is the only low-redshift, lobe-dominated source known to show a strong linear X-ray jet of the type seen in CDQs, and so provides a useful comparison object. PKS 0637–752 itself was excluded because it is not visible to the VLA. Some basic properties of the sample are given in Table 1.

For each object in the sample I retrieved the *Chandra* X-ray data for from the public archive. In some cases there was more than one observation, and here generally I simply used the longest: the aim here is to have sufficient statistics to make a flux measurement, rather than to make the best possible X-ray maps. The *Chandra* observation IDs and corresponding livetimes used are tabulated in Table 1. X-ray analysis was carried out using CIAO 3.2.1 and CALDB 3.0.0.

VLA data were used to obtain single-frequency radio maps with a resolution as closely matched to that of *Chandra* as possible. The images for 0605–085, 1136–135, 1150+497, 1354+195 and 1510–089, which were presented in Sambruna et al. (2004), were kindly made available to me by C. C. Cheung and are now available from the XJET web page. R. A. Perley provided me with images of Pic A from Perley, Röser & Meisenheimer (1997). I retrieved data for 0827+243, 1127–145 and 3C 273 from the public VLA archive [the first two datasets being the basis of the images presented in Jorstad & Marscher (2004) and Siemiginowska et al. (2002) respectively]. Where I retrieved VLA data from the archive myself, they were reduced in the standard manner using AIPS, with several iterations of self-calibration typically being used to improve the dynamic range.

Once X-ray data and radio maps were available, I divided each jet into a number of sub-regions, taking radio and X-ray measurements for each. The regions were defined in general on the basis of the X-ray images, since the separation into sections was limited by the X-ray signal-to-noise, but their dimensions were measured from the radio data. Because the number of counts from any given jet was small, I fitted a power-law spectrum with Galactic absorption to the whole jet for each source and used this spectrum to determine the conversion between counts in the 0.5–5.0 keV energy range and flux density. As this conversion factor is only a weak function of

**Table 1.** Properties of the sources in the sample

IAU name	Other name	$z$	$S_{1.4}$ (Jy)	$L_{1.4}$ (W Hz $^{-1}$ sr $^{-1}$ )	Reference	<i>Chandra</i> OBSID	Livetime (s)
0518–458	Pictor A	0.035	6.3	$1.4 \times 10^{24}$	1, 2	3090	36351
0605–085	PKS	0.870	1.9	$9.2 \times 10^{26}$	3	2132	8663
0827+243	B2	0.939	0.9	$5.4 \times 10^{26}$	4	3047	18268
1127–145	PKS	1.18	5.7	$6.7 \times 10^{27}$	5	866	27358
1136–135	PKS	0.554	4.3	$6.0 \times 10^{26}$	3, 8	3973	70174
1150+497	4C 49.22	0.334	1.6	$5.9 \times 10^{25}$	3, 8	3974	62122
1226+023	3C 273	0.158	53.6	$3.2 \times 10^{26}$	6, 7	4876	37457
1354+195	4C 19.44	0.720	2.6	$7.4 \times 10^{26}$	3	2140	9056
1510–089	PKS	0.361	2.7	$1.2 \times 10^{26}$	3	2141	9241

‘IAU name’ lists the (B1950-derived) positional name of the source. ‘Other name’ lists the name of the source in radio catalogues, if one is widely used. ‘PKS’ means that the source is taken from the Parkes catalogue and normally referred to with a PKS prefix; similarly, ‘B2’ implies a source from the second Bologna catalogue. Redshifts are taken from the XJET catalogue, which in turn generally takes them from the papers listed in the ‘Reference’ column. 1.4-GHz flux densities are taken from FIRST or NVSS maps, except for Pic A, where data from Perley et al. (1997) are used. Luminosities are calculated from the flux densities assuming a spectral index of 0.8. References give previously published discussions of the X-ray jet, and are as follows: 1, Wilson, Young & Shopbell (2001); 2, Hardcastle & Croston (2005); 3, Sambruna et al. (2004); 4, Jorstad & Marscher (2004); 5, Siemiginowska et al. (2002); 6, Marshall et al. (2001); 7, Sambruna et al. (2001); 8, Sambruna et al. (2005).

power-law index, this procedure should not introduce much uncertainty into the measurements. X-ray counts and radio flux densities were then measured from identical regions, with background subtraction where necessary (always for X-ray but only occasionally for radio). In a couple of cases there was no significantly detected radio emission from an X-ray region, and in this case an upper limit was determined from the off-source noise on the radio map. The X-ray counts were converted to a 1-keV flux density using the conversion factors determined from the spectral fitting. The length of the region, the typical jet radius within the region, and the distance of the region from the nucleus (measuring along the jet to the centre of the region) were also recorded. All these data for each region are tabulated in Table 2. A plot of the radio/X-ray spectral index,  $\alpha_{RX}$ , derived from these measurements is shown in Fig. 1; this illustrates the point that  $\alpha_{RX}$  generally increases with distance along the jet.

The radio and X-ray data were then modelled using a version of the code described by Hardcastle et al. (2002a) which numerically integrates the inverse-Compton equations set out by Brunetti (2000) in the rest frame of the jet, and then transforms back to the lab frame. This avoids the use of some of the analytical approximations adopted in the literature, which are strictly correct only in the limit  $\Gamma \gg 1$ . Each jet segment is taken to be a homogeneous cylinder with length and width determined by the measurements tabulated in Table 2. The modelling takes account of the fact that the inferred volume of the jet, which has a significant effect on the inverse-Compton emission, is dependent on the angle to the line of sight  $\theta$ . I follow Scheuer & Readhead (1979) in adopting  $S = S' \mathcal{D}^{(2+\alpha)}$  as the appropriate Doppler boosting formula for continuous jets emitting isotropically in their rest frames, and I assume that the rest-frame synchrotron emission is isotropic. I further assume, as is conventional, equipartition between electron energy and magnetic field, so that the radio data point provides the normalization for the electron energy spectrum, and that there are no energetically significant protons<sup>2</sup>. The electron energy spectrum is

assumed to be a power law with index  $p$  between electron Lorentz factors  $\gamma_{\min}$  and  $\gamma_{\max}$ . As discussed above (Section 1.2.3),  $\gamma_{\min}$  has to be  $\sim 10$  or lower to allow the CMB to be scattered by the jet and to avoid a flat or inverted spectrum in the X-ray.  $\gamma_{\max}$  is less important to the result so long as it corresponds to frequencies well above the lab-frame radio constraints.  $p$  would in principle be constrained by multi-frequency radio observations, but few of these are available. In what follows I assume  $p = 2.5$  (corresponding to a radio spectral index  $\alpha_R = 0.75$ ),  $\gamma_{\min} = 10$ , and  $\gamma_{\max} = 4 \times 10^5$ . I have verified that the choices of parameters do not have a strong effect on the qualitative results presented here, though clearly some changes can have a significant quantitative effect.

### 3 SAMPLE RESULTS

#### 3.1 Angles

There is a degeneracy between the angle to the line of sight  $\theta$  and the bulk Lorentz factor  $\Gamma$  required to produce a given amount of X-ray emission from the observed radio. The approach I take here is therefore to keep one fixed while varying the other (cf. Marshall et al. 2005). Ideally, we would know  $\theta$  for a given source independently, but for most of these sources there are no useful constraints. I began by keeping  $\Gamma$  fixed ( $\Gamma = 10$ , as used by Marshall et al.) and solving for the required  $\theta$  for each source and jet region. This showed that small angles to the line of sight ( $< 10^\circ$ ) are generally required, particularly at the bases of the jets, if the CMB/IC process is to account for the observed X-rays with plausible bulk Lorentz factors. The angle to the line of sight required for a fixed

radio sources and the energy densities in the electron population has to be a coincidence if there is an energetically dominant proton population. Since the kpc-scale jets directly feed the lobes and hotspots, this seems a reasonable inference. If there is a population of protons or other non-radiating particles with an energy  $\kappa$  times that of the electrons, and the magnetic field is in equipartition with the total energy density of the particles, then the inverse-Compton emissivity goes as  $(1 + \kappa)^{-\frac{p+1}{p+5}}$ , where  $p$  is the electron energy index discussed in the text: thus moderate contributions from protons, with  $\kappa \sim 1$ , make little difference to the results.

<sup>2</sup> The reason for the assumption of no energetically significant protons is that, as argued by Hardcastle et al. (2004) and Croston et al. (2005) for hotspots and lobes respectively, the similarity between the energy densities in the magnetic fields measured in the large-scale components of powerful

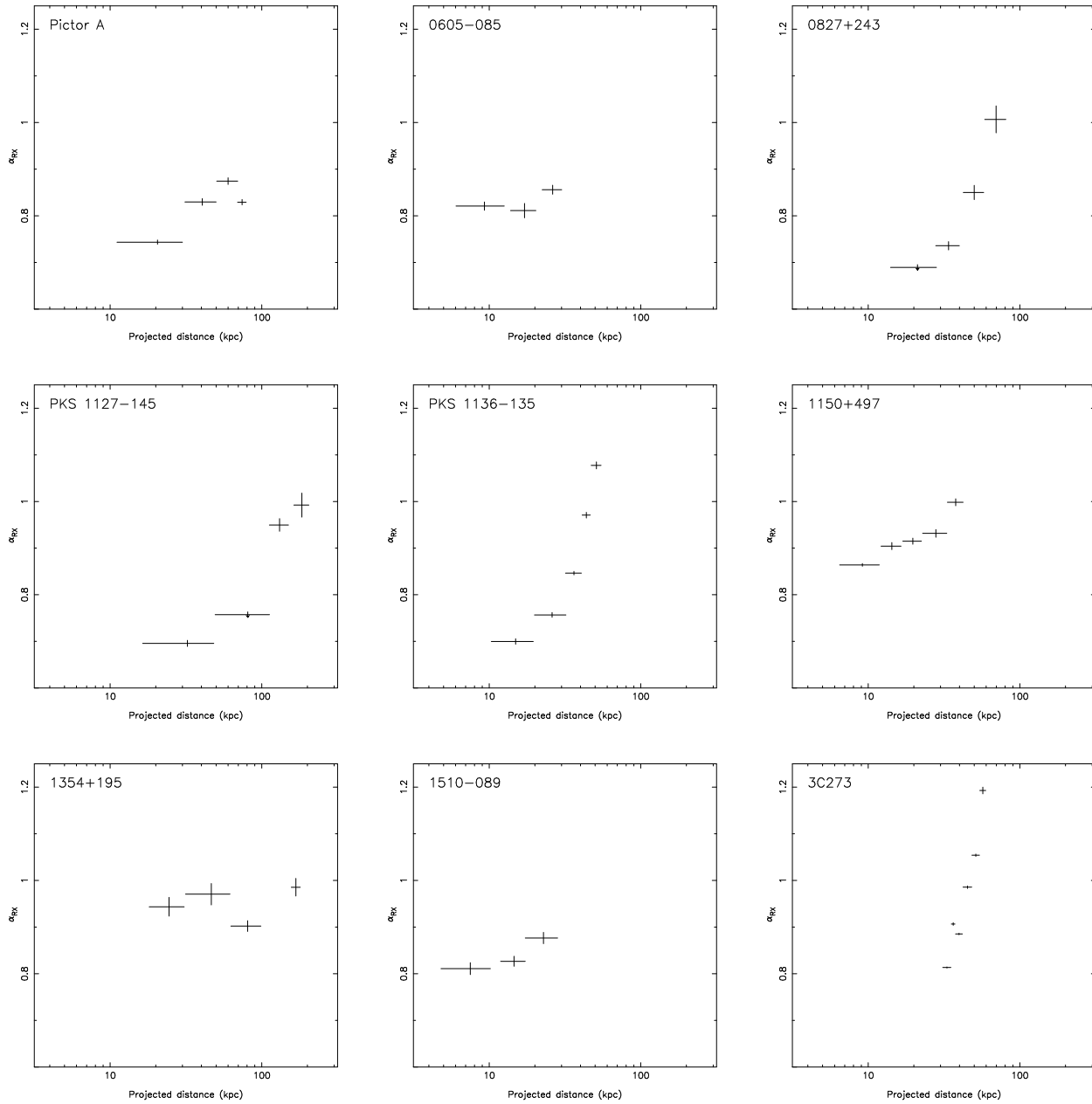


**Figure 1.** The two-point radio/X-ray spectral index of the jet components as a function of projected distance. Arrows indicate upper limits on  $\alpha_{RX}$ , resulting from upper limits on the radio emission.

$\Gamma$  increases systematically along the jets, as we would expect from Fig. 1: if this were true, it would imply that the jets were bending away from the line of sight. While this is not impossible – selection effects require that the jet be aligned close to the nucleus, but say nothing about what it should do further out – there is in general no evidence in the maps for jet bending of similar magnitude (tens of degrees) in the plane of the sky (though one source, 0827+243, does have a sharp bend of nearly  $90^\circ$  in projection). So a model in which angle changes are responsible for the change in radio/X-ray ratio seems implausible.

### 3.2 Lorentz factors

The more intrinsically probable model to test is the one in which the speed of the jet changes as a function of distance. I used the results of the previous subsection to choose a fixed angle,  $\theta = 4^\circ$ , that represents a compromise between extreme projection and the requirement that the CMB/IC model be able to produce the observed X-rays, and solved for  $\Gamma$  for each source component. The results are plotted for each source in Fig. 2. Errors are the statistical errors only, derived from the  $1\sigma$  (Poisson) errors on the measured jet X-ray flux densities, and no attempt is made to represent the (potentially large) systematic uncertainties due to inadequacies of the model. Some components are not plotted because a  $4^\circ$  angle to the line of sight does not allow the model to produce the observed X-rays from the measured radio emission: thus, for example, PKS

**Table 2.** Measurements from the regions used in the paper

Source	Freq. (GHz)	Distance (arcsec)	Length (arcsec)	Width (arcsec)	Radio flux (mJy)	X-ray flux (nJy)
Pictor A	1.4	29.8	27.4	2.0	6.5	5.0
		58.9	27.4	2.0	16.8	2.5
		86.9	27.4	2.0	38.7	2.5
		107.6	14.0	2.0	18.4	2.8
0605–085	4.9	1.4	1.0	0.3	11.1	5.3
		2.6	1.0	0.3	4.8	2.7
		4.0	1.2	0.6	19.1	4.9
0827+243	4.9	3.2	2.1	0.5	<0.5	2.7
		5.1	1.8	0.5	1.0	2.1
		7.6	2.3	0.5	3.7	1.1
1127–145	8.5	10.5	3.3	0.5	14.1	0.3
		4.8	4.7	0.5	0.4	2.7
		11.9	9.3	0.6	<0.7	1.6
		19.3	5.5	0.7	8.5	0.7
1136–135	4.9	27.0	6.2	0.8	10.4	0.4
		2.6	1.6	0.5	0.3	1.3
		4.6	2.2	0.5	1.2	1.8
		6.4	1.5	0.5	10.3	3.1
1150+497	4.9	7.7	0.9	0.5	38.3	1.3
		9.0	1.4	0.6	165.7	0.8
		2.1	1.2	0.2	28.4	6.3
		3.2	1.0	0.2	12.5	1.4
3C 273	4.8	4.5	1.3	0.2	16.0	1.5
		6.3	2.3	0.2	15.9	1.1
		8.6	2.0	0.9	50.5	1.0
		12.6	1.6	0.2	95.0	51.2
1354+195	4.9	13.9	0.8	0.7	77.0	7.9
		15.2	1.6	0.8	207.3	31.2
		17.3	2.3	1.2	549.4	14.0
		19.6	2.2	1.2	1979.6	14.9
		21.8	2.0	1.2	3138.3	2.0
		3.9	2.0	0.2	17.3	0.9
1510–089	4.9	7.5	4.9	0.2	33.4	1.1
		13.0	5.8	0.2	22.3	2.5
		27.0	3.7	1.5	50.8	1.3
1510–089	4.9	1.6	1.2	0.1	6.9	3.9
		3.2	1.2	0.2	8.3	3.6
		4.9	2.4	0.3	18.0	3.2

1510–089 only has one data point on the plot, corresponding to the outermost region of the jet. Similarly, some upper error bars are not plotted because the model cannot reproduce the whole  $1\sigma$  range possible from the X-ray data. In some cases the values I plot in Fig. 2 are significantly different from published values for the sources in question: I attribute this to a combination of a different approach (the use of a fixed  $\theta$ , as opposed to trying to determine it for each source), a different method (as discussed above) and, in a number of cases, different radio and/or X-ray data.

The trend seen in the plot for almost every individual source is clearly in the sense that lower bulk Lorentz factors are required at larger distances from the nucleus. The inner parts of the jet often require  $\Gamma \gtrsim 15$  while the outer parts typically have  $\Gamma \lesssim 5$ . Although the detailed numbers will depend on the actual angle to the line of sight, I verified using other values that the trend with distance does not.

### 3.3 Energy transport

Since the rest-frame energy density  $U$  and speed of the jet are determined by the fits, the lab-frame energy carried by the jet in the form of magnetic field and electrons,  $W = Ac\Gamma^2U$ , can be calculated, where  $A$  is the cross-sectional area and  $c$  the speed of light. The results of this calculation are plotted in Fig. 3: as in the previous section,  $\theta = 4^\circ$  is assumed. The value of  $W$  for a given jet component (unlike the Lorentz factor or angle) have a strong dependence on the assumed jet radius, which is hard to measure accurately. However, it is interesting that in many cases the power is approximately constant, within a factor of a few, which is certainly not the case for the quantity  $\Gamma^2$ ; this is consistent with what we might expect if the CMB/IC+deceleration model were correct. The powers implied by this calculation, which of course assumes no protons are present in the jet, are of the order of  $10^{38} - 10^{39}$  W (except in the case of the nearby Pic A), which are reasonable (cf. the jet powers derived on similar minimum-energy assumptions by Rawlings & Saunders 1991). They are comparable to the ‘luminosities’ estimated for the X-ray jets, but of course the emission from these is not isotropic in the CMB/IC model and so the true lab-frame luminosity is much lower. Except for the sources where there is a big change in the energy requirements along the jet, e.g. at the end of 1354+195, there is little here to provide evidence against the CMB/IC model. Note that the angle to the line of sight adopted means that some of the sources would be required to be very large. These sources (1127–145 and 1354+195 in particular) probably in reality have larger angles to the line of sight and would require correspondingly larger  $\Gamma$ .

Protons in the jets could well dominate the jet energetics while still being few enough, or cold enough, not to violate the assumptions set out in Section 2 about the nature of the internal energy density of the jet. There is no way of estimating the number of cold protons present in the jet but, to take one possible scenario, if there were the same number density of cold protons and energetic electrons, the energy transported would increase by two orders of magnitude. One possibly interesting point to make is that if protons dominate the energy transport, then we might expect the quantity plotted in Fig. 3 to increase with distance along the jet, as the jet decelerates and the bulk kinetic energy of the protons is translated into internal energy. If the deceleration model is correct, then the fact that this is not observed suggests that protons do not greatly dominate the energy transport on these scales.

## 4 DISCUSSION

### 4.1 Deceleration...

As the previous sections have shown, deceleration of jets, inferred by e.g. Georganopoulos & Kazanas (2004), is required by the data in the context of the simplest CMB/IC model, in which jets are homogeneous cylinders with uniform velocities. The deceleration takes place on scales of hundreds of kpc, comparable to the size of the radio lobes if we assume that these sources are normal classical double radio galaxies seen in extreme projection.

However, we already know from the speeds inferred from properties of kpc-scale jets (Section 1.2.1) that the most likely situation is that jets do not have uniform velocities. One of the most surprising implications of the deceleration model is that the fast spine of the jet (producing the X-rays in the CMB/IC model) must decelerate from  $\Gamma > 15$  to  $\Gamma < 5$  on 100-kpc scales without there being any evidence for such deceleration in the slower outer regions. No

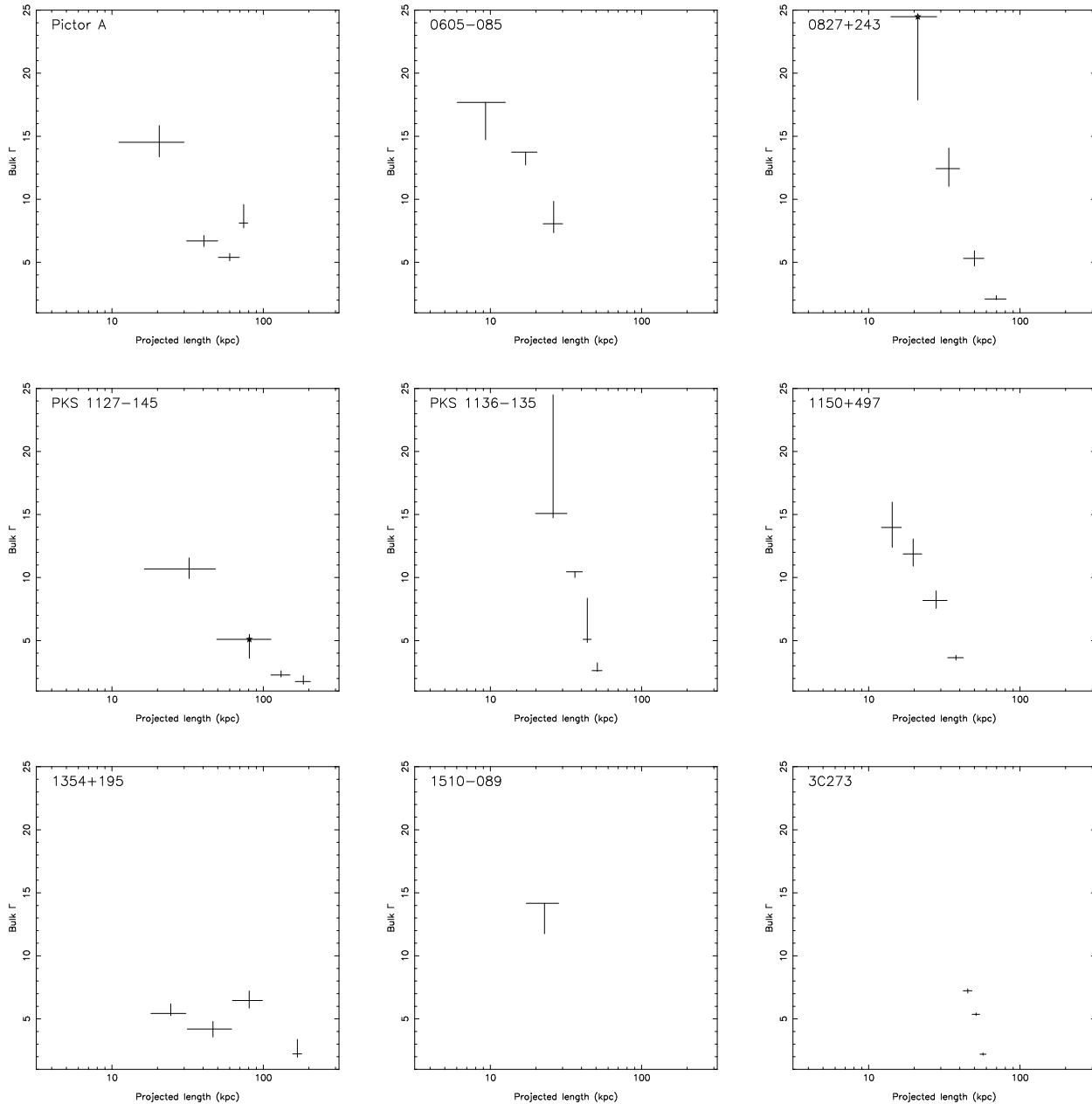


**Figure 2.** Inferred bulk Lorentz factor  $\Gamma$  as a function of projected length along the jet for the 9 sample sources, assuming  $\theta = 4^\circ$ .

tendency is observed in studies of FRII sources (e.g. Hardcastle et al. 1997, Gilbert et al. 2004, Mullin et al. in preparation) for the jets to become more two-sided, or more prominent, at large distances (at least until the jet enters the area of the hotspots). It is hard to see how, in this two-speed model of the jets, the slower material can retain its speed while the faster material decelerates, at least in any picture in which the deceleration is the result of some influence from outside the jet: the same is true of any more sophisticated model in which there is a continuous range of speeds in the jets. A detailed model of the deceleration process must explain this observation.

Another important question is the mechanism for deceleration. In FRI jets, the evidence for jet deceleration is overwhelming, in view of the transition between one-sided and two-sided jets on scales of a few kpc (see e.g. Laing & Bridle 2002). The physical

mechanism invoked for FRIs, in order to decelerate the jets while conserving their momentum, is entrainment of external material. It has been argued (e.g. Bowman, Leahy & Komissarov 1996) that a relativistic jet can entrain matter and undergo substantial deceleration without catastrophic dissipation of the energy flux of the jet (which we know cannot be the case in the quasars both from the results of Section 3.3 and from the fact that the jets do not generally become much more luminous at large distances). Bowman et al. argue that relativistic jets will not entrain efficiently via turbulence at a boundary layer, as they do in Bicknell’s (1984) model of transonic FRI jets: instead, they propose that mass loss from stellar winds into the jet is sufficient. This cannot be the case on the scales we are concerned with, however, for the deceleration is important on scales of hundreds of kpc, well beyond the scale at which there is a significant density of stars from the host galaxy. Setting this

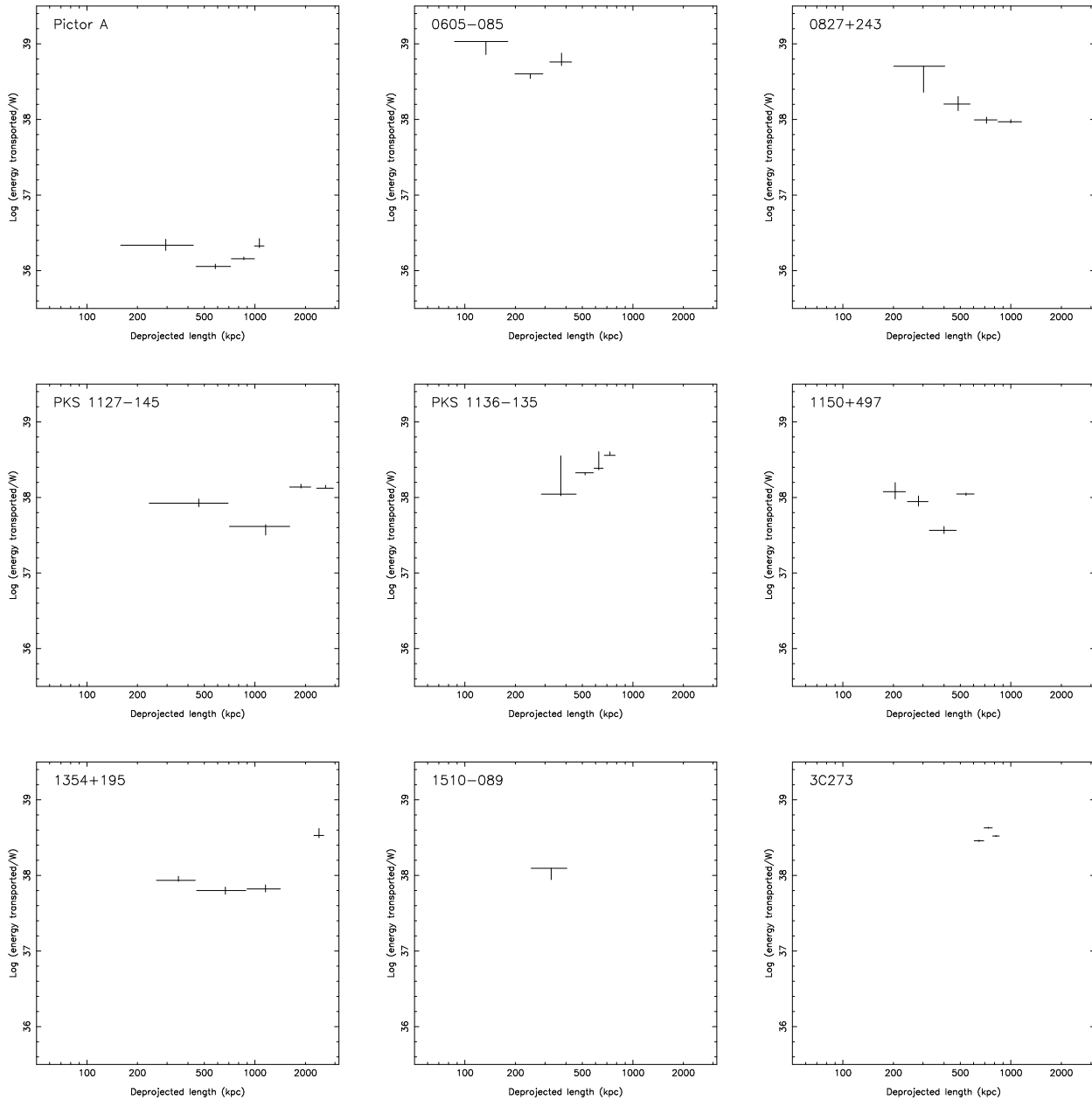


**Figure 3.** Inferred jet power (energy transport along the jet) as a function of deprojected distance along the jet assuming  $\theta = 4^\circ$ .

aside, let us suppose that entrainment injects cold, dense material into the jet. Momentum flux balance then would imply that the final bulk Lorentz factor would be controlled by the density of entrained material: if the jet is initially entirely composed of a relativistic fluid then we have, requiring momentum flux to be constant<sup>3</sup>,

$$\frac{\Gamma_i}{\Gamma_f} = \sqrt{\frac{A_f}{A_i} \left( \frac{U_f + \rho c^2}{U_i} \right)} \quad (1)$$

where subscripts  $f$  and  $i$  refer to the final and initial states respectively, and  $\rho$  is the density of entrained material in the final jet.

<sup>3</sup> Here we are assuming that the jet propagates through a constant-pressure cocoon, so that the term that arises due to the external pressure gradient (Bicknell 1994) may be neglected.

For significant deceleration the rest-frame energy density in the entrained material must be comparable to, or exceed, the energy density in relativistic particles, and this would require entrained masses of  $10^3$ – $10^4 M_\odot$  in regions at the end of the jet in the most extreme cases, which is certainly not possible by stellar wind entrainment, where only around  $1M_\odot$  is plausibly available (using mass loss rates from Bowman et al. 1996). If protons dominate the jet energy/momentum flux, the masses required are clearly higher. Some sort of boundary-layer entrainment might be possible, but runs into two further problems. Firstly, the energy densities of the relativistic material do not appear to decrease significantly, as implied by the results of Fig. 3: if a non-relativistic component were coming to dominate the momentum and so kinetic energy density of the source, the energy transported by relativistic particles should decrease markedly, but it does not. Secondly, any boundary-layer



process should presumably be particularly efficient in coupling the slow outer layers of the jet with the fast inner spine, and produce increasing two-sidedness of the kpc-scale jet in the more weakly beamed FR II radio galaxies and lobe-dominated quasars, which, as discussed above, is not observed.

The relative constancy of the energy transported by relativistic particles and field (Fig. 3) in fact suggests that the deceleration, if real, takes place by translating bulk kinetic energy into internal particle energy. One process that is worth considering, because it does not require any particular coupling between the slow and fast regions of the jet, is internal shocks in a jet composed of multiple sub-regions of different speeds (e.g. Spada et al. 2001). These shocks cause the Lorentz factor of the jet to tend to a constant value, rather than decreasing monotonically along the jet, but beaming effects mean that we would tend to see the inner parts of the jet as dominated by faster-moving material. However, in order to produce Lorentz factors as low as those calculated for the outer parts of the jet, the process generating the different regions ('shells', in the terminology of Spada et al.) would have to produce some with very low  $\Gamma$ , and considerable fine tuning would then seem to be required to make sure that the interactions happened on 100-kpc scales rather than the sub-pc scales discussed by Spada et al..

One positive point in favour of a deceleration model in the CMB/IC framework is that it helps to explain why Marshall et al. (2005) see little correlation between CMB/IC emission and  $(1+z)$ . If jets decelerate, then the variation in  $\Gamma^2$  alone is enough to wash out much of the dependence on rest-frame CMB energy density, setting aside other important sources of scatter such as source geometry and angle to the line of sight. On the other hand, permitting deceleration removes what was initially an attractive feature of the CMB/IC model, namely the apparent similarity between the jet speeds on pc and kpc scales (cf. Tavecchio et al. 2004).

#### 4.2 ... or something else?

As the discussion above shows, there are some potentially serious problems for a deceleration model in the CMB/IC framework. Can any other model explain the observations?

If we wish to retain an inverse-Compton origin for the X-ray emission, then one obvious possibility is to relax the assumption of equipartition of energy between the electrons and magnetic field. Although there is a good deal of evidence that the magnetic field strengths in the hotspots and lobes of FR II sources are close to the equipartition values [see, respectively, Hardcastle et al. (2004) and Croston et al. (2005) for discussions of the X-ray emission from these components] the inferred field strengths are generally slightly below the equipartition value. More importantly, as the mechanism by which the electrons and magnetic fields come into equipartition is not clear, there is no very strong reason to suppose that jets follow the pattern of lobes and hotspots. For the assumed model, a magnetic field that is lower than the equipartition value by a factor 2 (in terms of magnetic field strength) corresponds to an increase in the X-ray flux density of a factor  $\sim 3.5$ , or a change of 0.07 in radio/X-ray spectral index (Fig. 1): comparatively small departures from equipartition can have large effects on the observed X-rays. The obvious difficulty with this model is that there is no *a priori* reason for supposing that the magnetic field strength will vary in the required way. Nor is it obvious how this model could be tested. If we relax the assumption of equipartition, then we can produce the X-ray emission with bulk speeds much closer to the speeds estimated from the large-scale radio jet properties. Of course, with

large enough departures from equipartition, boosting of the CMB using large bulk Lorentz factors is not necessary at all.

The most obvious alternative model is that the X-ray emission is, at least partially, not inverse-Compton emission at all, but synchrotron radiation. Although CMB/IC is a required process, and must eventually come to dominate with increasing redshift, whether or not the bulk Lorentz factor is high, that does not necessarily imply that it is the process we see in the (mostly relatively nearby) objects discussed here. As I discussed in Section 1.2.2, the arguments against synchrotron models are not yet strong, and indeed synchrotron models have already been adopted for some of the bright inner knots of objects in the current sample (Sambruna et al. 2004), while there is an active controversy over the origin of the X-rays from 3C 273 (Marshall et al. 2001, Sambruna et al. 2001). Jester et al. (2002) have shown that the spectrum of components of the 3C 273 jet turns up in the infrared-ultraviolet wavelength range, so that a second spectral component is unambiguously required to be present: qualitatively, this is consistent either with a synchrotron model or with an inverse-Compton model with a suitably low  $\gamma_{\min}$ . We know (Section 1.1) that synchrotron emission is possible from the jets of FR II sources, though it should be noted that at present there is no unambiguous detection of synchrotron emission from the jet of a source comparable in luminosity to the core-dominated quasars in the present sample. Again, we have no detailed physical understanding of what might cause a change in the amount of X-ray synchrotron emission produced as a function of distance along the jet. However, it is worth noting that a very similar trend is seen in many FR I radio sources, and in such sources the jet emission is certainly synchrotron in origin. Occam's razor suggests that we should think very carefully about invoking two entirely different processes to describe such similar phenomena.

## 5 SUMMARY AND CONCLUSIONS

I have analysed a small heterogeneous sample of objects with known extended X-ray jets in the framework of the boosted CMB inverse-Compton ('CMB/IC') model originally set out by Tavecchio et al. (2000) and Celotti et al. (2001). Assuming that the CMB/IC process accounts for all the X-rays, that the jets can be modelled as homogenous cylinders, that the radio emission determines the geometry, and that equipartition between electrons and magnetic fields holds, I find that significantly lower speeds are required at larger distances from the nucleus in almost all of the sources studied, consistent with earlier suggestions (e.g. Georganopoulos & Kazanas 2004) but distinctly inconsistent with the idea that the parsec-scale speed is reproduced on the kpc scale (e.g. Tavecchio et al. 2004). Although the quantitative estimates of  $\Gamma$  presented are based on the assumption of a single angle to the line of sight, the qualitative picture is independent of that assumption.

From these observations the following conclusions can be drawn:

- The speeds required (in the objects studied here, and in general) are much larger than the speeds inferred from studies of the kpc-scale jets in lobe-dominated objects: thus, if the CMB/IC model is correct, jet velocity structure is almost certainly required.
- If the underlying assumptions are true, then deceleration is required, at least in some sources: but it is far from clear how the deceleration can take place, and there is no evidence for deceleration in the properties of lobe-dominated objects, which might be expected in a model where jet velocity structure was present.

• If deceleration is to be avoided, some other process must account for the decreasing X-ray/radio ratio along the jets. If the equipartition assumption is relaxed, then the observations can be modelled (admittedly in an entirely *ad hoc* way) in terms of a varying magnetic field/electron energy density ratio. If the assumption that CMB/IC is the only emission process is relaxed, and synchrotron radiation provides some or all of the X-rays, then the jets of the core-dominated quasars studied here have properties strikingly similar to those of the much lower-power FRI radio galaxies.

## ACKNOWLEDGEMENTS

An early version of this work was presented at the Banff meeting on Ultra-Relativistic Jets in Astrophysics (2005 July 11–15). I am grateful to the participants there, particularly Dan Harris, Robert Laing, Maxim Lyutikov, Hermann Marshall, Eric Perlman and Dan Schwartz, for constructive discussions of the physics of quasar jets, and to Judith Croston for helpful comments on the first draft of the paper. Any controversial or erroneous statements remaining in the paper are my responsibility, not theirs! Teddy Cheung kindly provided me with radio maps for some of the quasars in the sample and Rick Perley provided the maps of Pictor A. I am grateful to an anonymous referee for constructive comments that helped me to improve the paper. The National Radio Astronomy Observatory is a facility of the National Science Foundation operated under cooperative agreement by Associated Universities, Inc.

## REFERENCES

- Arshakian, T.G., Longair, M.S., 2004, *MNRAS*, 251, 727  
 Bicknell, G.V., 1984, *ApJ*, 286, 68  
 Bicknell, G.V., 1994, *ApJ*, 422, 542  
 Bietenholz, M.F., Hester, J.J., Frail, D.A., Bartel, N., 2004, *ApJ*, 615, 794  
 Bowman, M., Leahy, J.P., Komissarov, S.S., 1996, *MNRAS*, 279, 899  
 Bridle, A.H., Hough, D.H., Lonsdale, C.J., Burns, J.O., Laing, R.A., 1994, *AJ*, 108, 766  
 Brunetti, G., 2000, *Aph* 13 107  
 Celotti, A., Ghisellini, G., Chiaberge, M., 2001, *MNRAS*, 321, L1  
 Comastri, A., Brunetti, G., Dallacasa, D., Bondi, M., Pedani, M., Setti, G., 2003, *MNRAS*, 340, L52  
 Croston, J.H., Hardcastle, M.J., Harris, D.E., Belsole, E., Birkinshaw, M., Worrall, D.M., 2005, *ApJ*, 626, 733  
 Dermer, C.D., Atoyan, A.M., 2002, *ApJ*, 568, L81  
 Evans, D.A., Hardcastle, M.J., Croston, J.H., Worrall, D.M., Birkinshaw, M., 2005, *MNRAS*, 359, 363  
 Fanaroff, B.L., Riley, J.M., 1974, *MNRAS*, 167, 31P  
 Georganopoulos, M., Kazanas, D., 2004, *ApJ*, 604, L81  
 Georganopoulos, M., Kazanas, D., Perlman, E., Stecker, F.W., 2005, *ApJ*, 625, 656  
 Gilbert, G., Riley, J.M., Hardcastle, M.J., Croston, J.H., Pooley, G.G., Alexander, P., 2004, *MNRAS*, 351, 845  
 Hardcastle, M.J., 2001, *A&A*, 373, 881  
 Hardcastle, M.J., Croston, J.H., 2005, *MNRAS*, 363, 649  
 Hardcastle, M.J., Alexander, P., Pooley, G.G., Riley, J.M., 1997, *MNRAS*, 288, 859  
 Hardcastle, M.J., Alexander, P., Pooley, G.G., Riley, J.M., 1999, *MNRAS*, 304, 135  
 Hardcastle, M.J., Birkinshaw, M., Worrall, D.M., 2001, *MNRAS*, 326, 1499  
 Hardcastle, M.J., Birkinshaw, M., Cameron, R., Harris, D.E., Looney, L.W., Worrall, D.M., 2002a, *ApJ*, 581, 948  
 Hardcastle, M.J., Worrall, D.M., Birkinshaw, M., Laing, R.A., Bridle, A.H., 2002b, *MNRAS*, 334, 182  
 Hardcastle, M.J., Harris, D.E., Worrall, D.M., Birkinshaw, M., 2004, *ApJ*, 612, 729  
 Hardcastle, M.J., Worrall, D.M., Kraft, R.P., Forman, W.R., Jones, C., Murray, S.S., 2003, *ApJ*, 593, 169  
 Harris, D.E., 2004, To appear in the proceedings of the workshop: "Science with Wavelengths on Human Scales" (Santa Fe, NM; 8-11 Sep. 2004) (astro-ph/0410485)  
 Jester, S., Röser, H.-J., Meisenheimer, K., Perley, R., 2002, *A&A*, 385, L27  
 Jorstad, S.G., Marscher, A.P., 2004, *ApJ*, 614, 615  
 Kataoka, J., Stawarz, L., 2005, *ApJ*, 622, 797  
 Kraft, R.P., Hardcastle, M.J., Worrall, D.M., Murray, S.S., 2005, *ApJ*, 622, 149  
 Laing, R.A., Bridle, A.H., 2002, *MNRAS*, 336, 328  
 Marshall, H.L., et al., 2001, *ApJ*, 549, L167  
 Marshall, H.L., et al., 2005, *ApJS*, 156, 13  
 Perley, R.A., Röser, H.-J., Meisenheimer, K., 1997, *A&A*, 328, 12  
 Perlman, E.S., Wilson, A.S., 2005, *ApJ*, 627, 140  
 Rawlings, S., Saunders, R., 1991, *Nat*, 349, 138  
 Sambruna, R.M., Urry, C.M., Tavecchio, F., Maraschi, L., Scarpa, R., Chartas, G., Muxlow, T., 2001, *ApJ*, 549, L161  
 Sambruna, R.M., Gambill, J.K., Maraschi, L., Tavecchio, F., Cerutti, R., Cheung, C.C., Urry, C.M., Chartas, G., 2004, *ApJ*, 608, 698  
 Sambruna, R.M., Gliozzi, M., Donato, D., Maraschi, L., Tavecchio, F., Cheung, C.C., Urry, M., Wardle, J.F.C., 2005, *ApJ* in press (astro-ph/0511459).  
 Scheuer, P.A.G., Readhead, A.C.S., 1979, *Nat*, 277, 182  
 Schwartz, D.A., et al., 2000, *ApJ*, 540, L69  
 Siemiginowska, A., Bechtold, J., Aldcroft, T.L., Elvis, M., Harris, D.E., Dobrzycki, A., 2002, *ApJ*, 570, 543  
 Spada, M., Ghisellini, G., Lazzati, D., Celotti, A., 2001, *MNRAS*, 325, 1559  
 Stawarz, L., Sikora, M., Ostrowski, M., Begelman, M.C., 2004, *ApJ*, 608, 95  
 Tavecchio, F., Ghisellini, G., Celotti, A., 2003, *A&A*, 403, 83  
 Tavecchio, F., Maraschi, L., Sambruna, R.M., Urry, C.M., 2000, *ApJ*, 544, L23  
 Uchiyama, Y., Urry, C.M., Van Duyne, J., Cheung, C.C., Sambruna, R.M., Takahashi, T., Tavecchio, F., Maraschi, L., 2005, *ApJ*, 631, L113  
 Wardle, J.F.C., Aaron, S.E., 1997, *MNRAS*, 286, 425  
 Wilson, A.S., Yang, Y., 2002, *ApJ*, 568, 133  
 Wilson, A.S., Young, A.J., Shopbell, P.L., 2001, *ApJ*, 547, 740  
 Worrall, D.M., Birkinshaw, M., Hardcastle, M.J., 2001, *MNRAS*, 326, L7